Mon. Not. R. astr. Soc. (1985) **212,** 359–365

Structure of the Crab Nebula: intensity and polarization at 20 cm

T. Velusamy *Radio Astronomy Centre, Tata Institute of Fundamental Research, PO Box 8, Ootacamund 643 001, India*

Accepted 1984 August 14. Received 1984 June 25.

Summary. VLA maps of the Crab Nebula at 20 cm with high dynamic range and resolution 15×15 arcsec^2 are presented. These maps show enhanced radio emission associated with optical filaments and an excellent correlation between depolarization at 20 cm and the bright optical filaments on the near side of the nebula. The overall structure of the radio emission is discussed, in particular the possibility that a circum-nebular remnant shell coincides with the outer boundary of the Crab Nebula.

1 Introduction

Recent optical observations of the filaments of the Crab Nebula (e.g. Chevalier & Gull 1975; Davidson 1978; Clark *et al.* 1983) lead to a picture in which the nebula consists of a inner shell of dense and bright filaments and an outer shell of thin fainter filaments. These inner and outer filaments have velocity and abundance differences. It might be possible to interpret these differences in terms of a type II supernova model (Chevalier 1977) in that, while the inner shell is influenced by the pulsar, the high-velocity outer shell is the ejected envelope of the supernova. Although there is some indication of an optical and X-ray halo around the nebula (Murdin & Clark 1981; Toor, Palmieri & Seward 1976), there is no evidence for a radio shell outside the nebular boundary (Wilson & Weiler 1982; Velusamy 1984). From the variation of the radio spectrum over the nebula, Velusamy & Sarma (1977) have nevertheless suggested that the radio emission close to the outer boundary of the nebula originates from the expanding remnant shell typical of other SNRs, and that the emission within the nebula originates from the electrons generated by the pulsar. In the inner parts of the Crab Nebula, enhanced radio emission associated with the bright optical filaments has been observed (Wilson 1972a). The large depolarization between 6 and 11 cm (Wilson 1972a; Swinbank 1980) as well as that at 21 cm (Duin & van der Laan 1972) is known to be caused by the filaments along the line-of-sight, particularly by those on the near side of the nebula. In this paper we examine the overall structure of the Crab Nebula and discuss the intensity and polarization associated with the bright optical filaments, using recent VLA observations.

2 Observational data

The 20-cm maps of the Crab Nebula discussed here were observed with the VLA in 1983 April and the observations have been described by Velusamy (1984; hereafter Paper I). The maps were made with the C-configuration data and a shortest spacing of 100λ. The dynamic range in this self-calibrated VLA map was about 1000. The resolution was 15×15 arcsec^2 at 20 cm. A contour map of total intensity highlighting and low surface brightness emission in the nebula, and a vector map of distribution of linearly polarized intensity and position angle, were published in Paper I. In order to bring out the structural details relevant for the discussion here, we have shown in Fig. 1 a total intensity map at 20 cm with appropriate choice of contour levels, and a vector map of the distribution of polarized emission. The photographic representations of these maps are shown in Plate 1, along with the interference filter photograph of the Crab Nebula in [O III] reproduced from Chevalier & Gull (1975).

3 Discussion

The 20-cm VLA map (Fig. 1) is consistent with earlier maps at 11 and 6 cm obtained with better resolutions by Swinbank & Pooley (1979) and Wilson (1972a). Because of the inclusion of shorter spacings and the large dynamic range, however, the VLA map reveals structures at very low brightness (<1 per cent of peak). The most prominent of these is the faint radio emission associated with the optical jet along the northern boundary, first detected by van den Bergh (1971) and discussed in Paper I. As seen in Fig. 1b, the degree of linear polarization and its position angle vary considerably over the nebula, the degree of polarization being nearly zero at several places. In general, there is a tendency for stronger polarization (10 to 20 per cent) in the outer regions, while the strongest polarization (~30 per cent) is in the northern jet.

3.1 A CIRCUM-NEBULAR SHELL?

As discussed in Paper I and by Wilson & Weiler (1982) there is no evidence for any large radio shell within 30 arcmin of the Nebula. The upper limit to the surface brightness for any shell is $\Sigma(1.4\,\mathrm{GHz})<0.6\times10^{-20}\,\mathrm{W\,m^{-2}\,Hz^{-1}\,Sr^{-1}}$, a value much lower than that expected for any supernova remnant shell that may be associated with the Crab Nebula. The haloes suggested by the optical (Murdin & Clark 1981) and X-ray (Toor *et al.* 1976) data may not represent a remnant shell, as they can be interpreted in other ways, for example as scattering of the nebular emission by interstellar dust. We can therefore rule out the presence of any remnant shell outside the nebular boundary. Nevertheless, in Chevalier's model for the Crab Nebula an expanding remnant shell is assumed and the outer filaments in the nebula might represent this expanding envelope (Chevalier 1977; Clark *et al.* 1983). Also Velusamy & Sarma (1977) have suggested the possibility that the radio emission along the boundary originates in the expanding remnant shell, in contrast to the emission within the nebula originating from the electrons generated by the pulsar. The VLA maps presented here provide some additional support for this interpretation.

Over the inner region (inside the second thick contour in Fig. 1a) the total intensity distribution shows highly filamentary structure superimposed on centrally peaked emission. The emission outside this region, on the other hand, is fairly smooth, particularly for brightness in the range 100 to 2000 mJy beam^{-1} (outer-shell). It may be that this region is the remnant shell associated with the expanding shock. The lack of limb-brightened radio structure as in other SNRs may be due to the stronger radio emission originating from the pulsar-generated relativistic electrons. Thus we may assume that a significant fraction of the emission in the outer region originates in the shell. Since the origin of the relativistic electrons in an outer-shell is likely to be different from that generated by the pulsar, some differences in radio spectrum between the inner and outer parts of

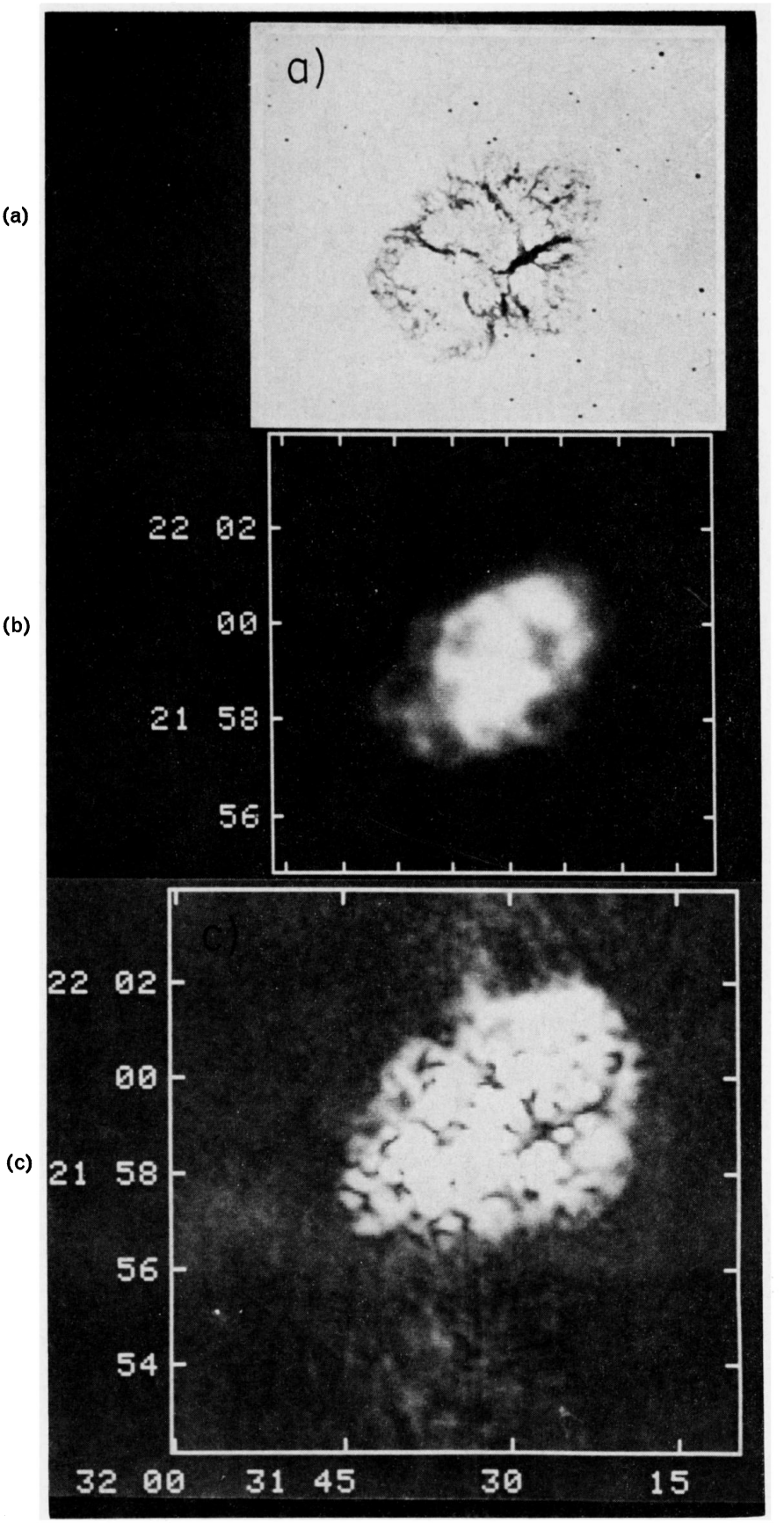

Plate 1. (a) Interference filter photograph of the Crab Nebula in [O III] λ5007 indicating the filamentary structure. Reprinted courtesy of Chevalier & Gull and the *Astrophysical Journal*, published by the University of Chicago Press; © 1975 The American Astronomical Society. (b) Photographic representation of the total intensity at 20 cm for brightness above 2000 mJy beam^{-1}. (c) Photographic representation of linearly polarized intensity at 20 cm, for brightness from 0 to 610 mJy beam^{-1}.

[*facing page* 360]

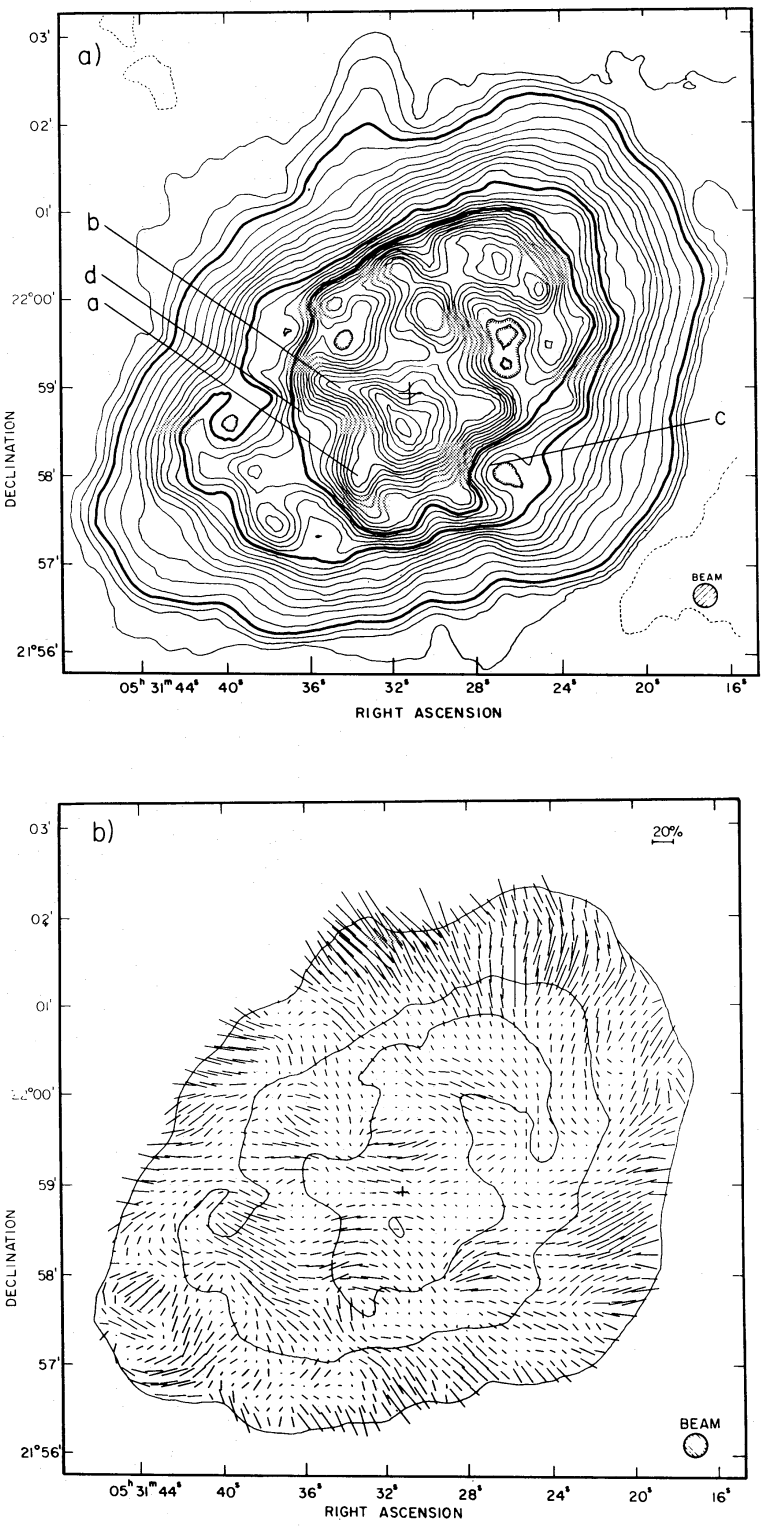

Figure 1. (a) Contour map of total intensity at 20 cm. Half-power beam width (15×15 arcsec^2) is shown by the hatched circle. The coordinates are for epoch 1950 throughout this paper. The cross marks the position of the pulsar. Contours are 10, 25, 50, 100, 200, and then increasing with interval of 200 to a maximum 6200 mJy beam^{-1}. The thick contours are at 100, 2000, 3000 mJy beam^{-1}. Negative values are indicated by dashed contours. Hatched contours represent local minima. The second thick contour at 2000 mJy beam^{-1} level roughly marks the inner boundary of the outer-shell (see text). (b) Linear polarization vectors at 20 cm. The degree of polarization and position angle of the *E*-vectors of the polarized emission are indicated by the length and orientation of the vectors. The contours are at 100, 2000, and 3800 mJy beam^{-1}. The vectors are drawn every 8 arcsec.

the Crab would be expected. In general the shell-type SNRs have steeper spectra, $\alpha>0.4$ (where $S_\nu \sim \nu^{-\alpha}$), than those with filled centres, e.g. $\alpha \sim 0.26$ for the integrated radio spectrum of the Crab. Velusamy & Sarma (1977) have observed that the spectrum is flat and remarkably constant over the inner parts and is steep only near the outer parts of the Crab. A comparison of the VLA map at 20 cm with Wilson's (1972a) 6-cm map (smoothed to the VLA resolution) shows a similar tendency for steepening on the spectrum in the outer-shell region, particularly in its eastern parts. One has to be careful in interpreting such results, however, in view of the absence of short spacings in the synthesis maps. A detailed study of the variation in the radio spectrum over the Crab, using high dynamic range maps obtained with equivalent $u-v$ coverage at all frequencies, would be very valuable.

The magnetic field in the inner parts of the Crab around the pulsar seems to be wound up by the pulsar (Rees & Gunn 1974), whereas the magnetic field in the outer-shell would be the compressed interstellar field (e.g. van den Laan 1962) or that amplified by instabilities (e.g. Gull 1973). One might therefore see differences in the magnetic field structure between the inner and outer parts of the Crab. The structure of the magnetic field in the inner parts has been well studied from optical (Woltjer 1957) and radio (Wilson 1972a) polarization. We know little about the magnetic field in the outer-shell. In Fig. 1b, a high degree of polarization (10 to 20 per cent) is seen over the outer parts along the boundary, and the electric vectors in general appear to be radial. Unlike the inner parts, the internal Faraday depolarization and rotation would be negligible for the outer regions. Assuming a uniform interstellar rotation measure of $-40\,\mathrm{rad\,m^{-2}}$, as for PSR 0525+21 (Manchester 1972), the Faraday rotation at 20 cm is $-90°$ and the orientations of the polarization vectors over the outer parts in Fig. 1b are then consistent with a radial projected magnetic field as in other young SNRs like Tycho's (Kundu & Velusamy 1971; Duin & Strom 1975) and Cas A (Rosenberg 1970). Thus both spectrum and polarization of the outer parts of the Crab seem to be consistent with those for an expanding remnant shell.

Although the presence of such a shell in the Crab Nebula seems possible, there are still difficulties in interpreting it as the radio shell associated with the shock front of the expanding envelope of the supernova. The extent of the radio emission (up to 1 per cent of the peak in Fig. 1a) is 452×336 arcsec^2 at a pa of 150°. The radio extent is consistent with the optical [O III] image of size 435×335 arcsec^2 (Gull & Fesen 1982). As shown in Paper I, the radio boundary extends beyond the optical image only in the north-western part along the major axis. Thus the maximum size of the shell is only 4.4×3.2 pc^2, assuming a distance of 2 kpc (Trimble 1973). Such a small diameter for the shell is not consistent with the Σ–D relation for SNRs of similar age (Clark & Stephenson 1977) and implies very low values for the initial expansion velocity and energy of the supernova. On the other hand, it is possible to interpret the shell as the result of interaction of the relativistic gas from the pulsar with the surrounding interstellar medium. Model computations by Chevalier (1984) show that, in the early stages of the evolution, such an interaction leads to formation of expanding shells of shocked gas. The radio emission from such a shell will have characteristics of a young shell-type SNR. Since the velocity and energy of the shell is determined by the pulsar wind, it need not be consistent with the Σ–D relation or the initial velocity of the supernova.

3.2 FILAMENTARY STRUCTURE

The radio emission in the inner parts of the Crab Nebula is due to the synchrotron radiation from relativistic electrons generated by the pulsar, moving in the magnetic field wound up by the pulsar. Within the optical filaments, both the density of these relativistic electrons and the strength of the magnetic field are likely to be increased by compression. Thus an enhanced emission will be observable from the optical filaments at radio wavelengths. Radio emission from

the filaments has been discussed by Swinbank (1980) and Wilson (1972b) based on observations at 11 and 6 cm. The VLA map at 20 cm provides additional data on these filamentary structures.

The radio photography of the total intensity at 20 cm in Plate 1b shows a good correlation between the bright optical filaments and regions of enhanced emission within the nebula. The correlation is very striking for the filaments seen along the outer boundary of the optical nebula. The inner filaments are also seen, but less clearly because of the poor resolution (15 arcsec) and the stronger radio emission over the central region. All of these filamentary features lie within the second thick contour in Fig. 1a. These features have also been seen in the high-frequency maps at 6 and 11 cm with resolutions of 6×16 and 4×11 arcsec^2 respectively by Wilson (1972a) and Swinbank & Pooley (1979). Indeed there is remarkable similarity between the filamentary structures in 6 and 20 cm maps, indicating little variation in the radio spectrum among the filaments.

In addition to observing the filaments directly by their radio emission, they can be studied indirectly by their influence on the nebular radio emission. For example, a filament with $N_e\sim1000\,\mathrm{cm}^{-3}$, $B\sim5\times10^{-4}$ G and a thickness ~0.01 pc will have Faraday rotation of 160 rad at 20 cm and only 15 rad at 6 cm. Such a large rotation, causing differential rotation of about 3 rad over the 12.5-MHz bandwidth used for the VLA observations, or any dispersion in the rotation across the filament would be sufficient to depolarize the radiation traversing a filament (Burn 1966; Velusamy & Kundu 1975). The correlation between depolarization at 11 cm and bright filaments has been studied by Wilson (1972a) and Swinbank (1980), but a stronger correlation is expected at longer wavelengths. Although Duin & van der Laan (1972) have measured the depolarization at 21 cm in the WRST map, their resolution (24×65 arcsec^2) is too low to resolve the contribution from the individual filaments. The high-resolution (15×15 arcsec^2) VLA map of the polarized intensity (Plate 1c) shows good correlation between the regions of low polarization and bright filaments, more clearly than any of the previous radio observations.

Only filaments located on the near side of the nebula depolarize the radiation seen through them. This can be seen clearly from a comparison of the distribution of polarized and total intensities across the filaments a and b in Fig. 1. Each filament shows enhanced emission in total intensity, but the polarized emission increases over the filament 'a' located on the far side (with +ve velocity), and decreases to nearly zero over the filament 'b' located on the near side (with −ve velocity). In Fig. 2 we have plotted the contours of degree of polarization at 20 cm superimposed on the bright optical filaments. The optical data for the filaments were taken from

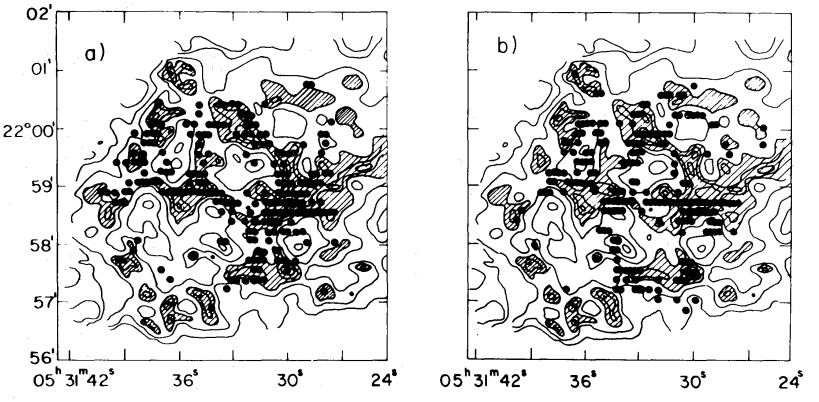

Figure 2. Distributions of bright optical filaments superimposed on the observed degree of linear polarization at 20 cm. The contours are at 0.5, 1, 2, 4, 8, 12, 16 per cent. The hatched areas indicate regions of low polarization less than 2 per cent. The dots represent bright optical filaments: (a) having negative velocities (located on the near side of the nebula), and (b) having positive velocities (located on the far side of the nebula). The data for the bright filaments were taken from Clark *et al.* (1983).

Clark *et al.* (1983). The shaded areas in Fig. 2 represent regions of lowest polarization, that is, highest depolarization, and these coincide remarkably well with the filaments having −ve velocity (Fig. 2a). The correlation between depolarization and filaments with +ve velocities is very marginal (Fig. 2b) and may not be significant, since some of these regions contain filaments with both −ve and +ve velocities. Thus it is clear that the low polarization (<2 per cent) at 20 cm over several regions in the nebula is due to the Faraday depolarization caused by filaments on the line-of-sight.

In general, a high degree of polarization (~10 per cent) is seen in the inner parts of the nebula over regions where the line-of-sight does not pass through any filaments. For example in region 'c' in Fig. 1 the degree of polarization is about 12 per cent. The rotation of the polarization between 20, 11 and 6 cm corresponds to a rotation measure of -28 ± 3 rad m^{-2}, which is also consistent with the mean rotation measure of -25 rad m^{-2} for the nebula (Wilson 1974). As an exception, very low polarization is seen over 'd' in Fig. 1, although there is no filament in this area. But it coincides with the eastern bay in the optical continuum map (Woltjer 1957). The high depolarization at 20 cm is consistent with the interpretation that this bay is associated with the region of thermal gas with lower densities in the range 10 to 30 cm^{-3} but with a larger extent of about 0.3 pc (Wilson 1974).

We have shown in Fig. 3 a sketch of the distribution of filaments on the near side of the nebula as obtained from the polarization on 20 cm. The surface area A of the nebula covered by these filaments is 6800 arcsec^2 or 0.64 pc^2. Faraday rotation at 20 cm is given by

$$\left(\frac{R}{\text{rad}}\right) = 0.032 \left(\frac{N_e}{\text{cm}^{-3}}\right)\left(\frac{L}{\text{pc}}\right)\left(\frac{B_\parallel}{\mu\text{G}}\right),$$

where N_e is electron density, L is distance through the filament along the line-of-sight and $B_\parallel$ is the longitudinal component of magnetic field in the filament. It is possible to estimate some of the physical parameters of the filaments from the Faraday rotation. For example, assuming $N_e \sim N_p$, the total mass in the filaments is given by

$$\frac{M}{M_\odot} \sim .76 \frac{AR}{B_\parallel}.$$

If the depolarization is caused by differential rotation within the bandwidth of 12.5 MHz at 1.4 GHz, the required Faraday rotation in the filaments is $R \sim 160$ rad. For $B \sim 2\times10^{-4}$ G (Wilson

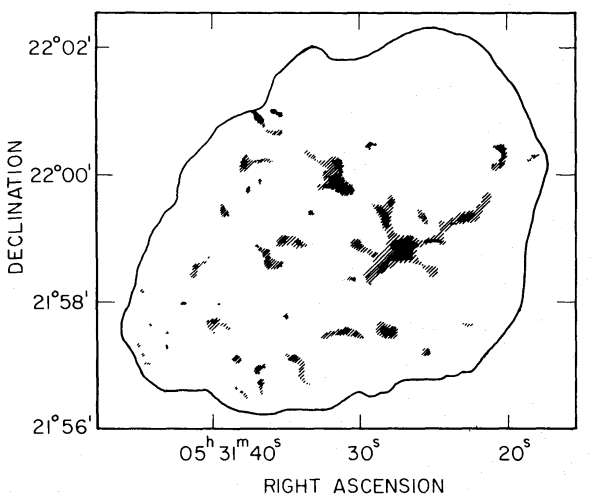

Figure 3. A sketch of the filaments on the near side of the nebula as derived from the polarization data at 20 cm. The contour indicates the 20-cm radio boundary.

1974), $M \sim 0.39\,M_\odot$. Thus, including a similar mass for those on the far side of the nebula, the total mass in the filaments is $\sim 0.78\,M_\odot$. We have considered only bright filaments causing high depolarization (observed polarization <1 per cent at 20 cm), but there are regions with significant depolarization and observed polarization $\lesssim 2$ per cent at 20 cm, which may be associated with fainter filaments. The above estimate of $0.78\,M_\odot$ is that only a lower limit to the mass in the filaments. It is very interesting that our estimate from radio depolarization is consistent with the limit $\geqslant 1.2\,M_\odot$ obtained from optical studies of the filaments (Henry & MacAlpine 1982). Indeed an extensive study of the individual filaments using both optical and high-resolution (a few arcsec) multifrequency (1.4 to 5 GHz) radio observations would be very valuable, to derive the physical conditions in the filaments more reliably.

Acknowledgments

The VLA of the National Radio Astronomy Observatory is operated by Associated Universities Incorporated under contract with NSF. I thank Drs Pramesh Rao and Swarup for comments.

References

Burn, B. J., 1966. *Mon. Not. R. astr. Soc.*, **133,** 67.
Chevalier, R. A., 1977. *Supernovae*, p. 53, ed. Schramm, D. N., Reidel, Dordrecht, Holland.
Chevalier, R. A., 1984. *Astrophys. J.*, **280,** 797.
Chevalier, R. A. & Gull, T. R., 1975. *Astrophys. J.*, **200,** 399.
Clark, D. H. & Stephenson, F. R., 1977. *The Historical Supernovae,* p. 207, Pergamon Press, Oxford.
Clark, D. H., Murdin, P., Wood, R., Gilmozzi, R., Danziger, J. & Furr, A. W., 1983. *Mon. Not. R. astr. Soc.*, **204,** 415.
Davidson, K., 1978. *Astrophys. J.*, **220,** 177.
Duin, R. M. & van der Laan, H., 1972. *Astrophys. Lett.*, **12,** 1977.
Duin, R. M. & Strom, R. G., 1975. *Astr. Astrophys.*, **39,** 33.
Gull, S. F., 1973. *Mon. Not. R. astr. Soc.*, **161,** 47.
Gull, T. R. & Fesen, R. A., 1982. *Astrophys. J.*, **260,** L75.
Henry, R. B. C. & MacAlpine, G. M., 1982. *Astrophys. J.*, **258,** 11.
Kundu, M. R. & Velusamy, T., 1971. *Astrophys. J.*, **163,** 321.
Manchester, R. N., 1972. *Astrophys. J.*, **151,** 43.
Murdin, P. & Clark, D. H., 1981. *Nature,* 294, 543.
Rees, M. J. & Gunn, J. E., 1974. *Mon. Not. R. astr. Soc.*, **167,** 1.
Rosenberg, I., 1970. *Mon. Not. R. astr. Soc.*, **151,** 109.
Swinbank, E., 1980. *Mon. Not. R. astr. Soc.*, **193,** 451.
Swinbank, E. & Pooley, G., 1979. *Mon. Not. R. astr. Soc.*, **186,** 775.
Toor, A., Palmieri, T. M. & Seward, F. D., 1976. *Astrophys. J.*, **207,** 96.
Trimble, V., 1973. *Publs. astr. Soc., Pacif.*, **85,** 579.
van den Bergh, S. 1971. *Astrophys. J. Lett.*, **160,** L27.
van den Laan, H., 1962. *Mon. Not. R. astr. Soc.*, **136,** 219.
Velusamy, T., 1984. *Nature,* **308,** 251 (Paper I).
Velusamy, T. & Kundu, M. R., 1975. *Astr. Astrophys.*, **41,** 307.
Velusamy, T. & Sarma, N. V. G., 1977. *Mon. Not. R. astr. Soc.*, **181,** 455.
Wilson, A. S., 1972a. *Mon. Not. R. astr. Soc.*, **157,** 229.
Wilson, A. S., 1972b. *Mon. Not. R. astr. Soc.*, **160,** 373.
Wilson, A. S., 1974. *Mon. Not. R. astr. Soc.*, **166,** 373.
Wilson, A. S. & Weiler, K. W., 1982. *Nature,* **300,** 155.
Woltjer, L., 1957. *Bull. astr. Inst. Neth.*, **13,** 301.